Artificial Neural Network (ANN)-based Crack Identification in Aluminum Plates with Lamb Wave Signals

YE LU,[1,2] LIN YE,[1,*] ZHONGQING SU,[2] LIMIN ZHOU[2] AND LI CHENG[2]

[1]*Laboratory of Smart Materials and Structures (LSMS), Centre for Advanced Materials Technology (CAMT) School of Aerospace, Mechanical and Mechatronic Engineering, The University of Sydney, NSW 2006, Australia*

[2]*Department of Mechanical Engineering, The Hong Kong Polytechnic University, Hong Kong SAR, China*

ABSTRACT: An inverse analysis based on the artificial neural network technique is introduced for effective identification of crack damage in aluminum plates. The concepts of digital damage fingerprints and damage parameter database, which are prerequisites for neural network developing and training, are presented. Parameterized modeling for finite element analysis and an information mapping approach are applied to constitute the damage parameter database cost-effectively. The generalization performance of the neural network is examined by a process of 'leave-one-out' cross-validation and diverse factors are discussed, based on which the optimization of the neural network architecture is evaluated. The capability of this inverse approach is assessed by two crack cases from experiments, with good accuracy obtained in damage parameters (central position, size, and orientation).

Key Words: Lamb waves, artificial neural network, damage detection, digital damage fingerprints.

INTRODUCTION

THE artificial neural network (ANN) technique is a promising solution for effective damage identification as a typical nonlinear inverse problem. Various changes in the characteristics of structural dynamic/static signals associated with damage have been employed for network training because they are easy to capture and sensitive to the existence of damage in some cases. These parameters include modal shapes and frequencies (Chang et al., 2000; Suh et al., 2000; Yun and Bahng, 2000; Ni et al., 2002; Yuan et al., 2003), displacement (Xu et al., 2001), velocity (Xu et al., 2004), and strain (Kudva et al., 1992; Shaw et al., 1995; Hwu and Liang, 2001). For identification of crack damage, Mahmoud and Kiefa (1999) input the first six natural frequencies into a neural network to estimate the location and size of surface cracks (15% deeper than the beam depth) in a steel cantilevered beam. Using natural frequencies and modal shapes as input patterns, Choubey et al. (2006) determined the size and location of through-thickness cracks which were 30% larger than the effective length of vessel structures. Liu et al. (2002) validated the feasibility of the ANN technique for crack detection using the responses of surface displacement. However, it is understood in general that initial or local damage leads to less detectable or undetectable changes in global structural dynamic parameters at low frequencies, which, as input vectors, compromise the performance of the ANN technique (Su, 2004).

Lamb waves propagating through damaged plate-like structures carry characteristics that can be correlated with the location and severity of a defect, providing another set of information for effective damage evaluation. For example, forward estimation of crack parameters (location, size, and orientation) and their effects on Lamb wave propagation have been extensively investigated in previous studies. It has been observed that, with an increase in excitation frequency, the value of the reflection coefficient of Lamb waves approaches a plateau of crack depth to plate thickness for surface-breaking cracks, and of crack length to plate width for through-thickness cracks (Lowe, 1998; Lowe and Diligent, 2002). Similar results have also been obtained in pipes for the reflection of the fundamental torsional mode by notches and cracks of different depths and circumferences in a frequency range of 0.01–0.3 MHz (Demma et al., 2003). However, a single actuator/sensor pair might be appropriate for evaluating only one crack parameter in simple cases, and crack size and orientation cannot be determined simultaneously with certainty because different cracks may show the same reflection/transmission coefficient, resulting in an incorrect judgment (Lu et al., 2007, 2008). As an inverse problem, it is difficult to employ these characteristics directly from

*Author to whom correspondence should be addressed.
E-mail: l.ye@usyd.edu.au
Figures 1 and 7 appear in color online: http://jim.sagepub.com

1045-389X/09/01 039–11 $10.00/0 DOI: 10.1177/1045389X07088782

scattered waves for quantitative determination of multiple parameters of damage (Xu et al., 2001).

Based on these observations, Su and Ye (2005a,b) assessed the location and size of hole and delamination damage in composite laminates using the ANN technique with the unique concepts of digital damage fingerprints (DDFs) and damage parameter database (DPD). An active sensor network was used for cross-examining the Lamb wave signals scattered by damage to bridge the implicit relation between damage parameters and unique characteristics in acquired signals using an ANN model as a typical inverse analysis.

In this study, the ANN technique for quantitative crack identification in aluminum plates was developed with the aid of DDFs verified by experiments. Parameterized modeling was adopted for finite element analysis (FEA) to effectively generate crack scenarios with randomly selected parameters. The information mapping technique (Su and Ye, 2005a,b) was applied to constitute the DPD of interest, which comprised extracted DDFs from the sensor network. The configuration of the proposed ANN was also optimized, based on evaluation of generalization performance with a process of cross-validation.

CRACK CASES FOR EXAMINATION

In this study, a $500 \times 500\,\text{mm}^2$ aluminum plate (1.6 mm in thickness) with encastre boundary condition was considered. It is assumed that the structure and material properties are isotropic in the plate without any prestress. Any changes in the propagation characteristics of Lamb waves are therefore correlated with the existence of damage only. Sufficient crack scenarios for ANN training can be developed by numerical simulation to replace the need for a large amount of experiments. However, under most circumstances, FEA software currently available can provide only a single modeling interface for a specific geometry. Such a procedure is extremely onerous and repetitive with various geometric parameters, since the whole system has to be remodeled. This concern becomes more serious when the damage parameters involved are also changed. For effective model construction with minimal effort, a parameterized modeling program was applied with the PATRAN command language (PCL)® (Huang et al., 2004).

Four PZT actuators/sensors were simulated on the upper surface of the specimen at positions illustrated in Figure 1, which can be recognized as a standard unit of an active sensor network. Crack cases were distributed in four sensor-enclosed quadrants (Zones I–IV in Figure 1), with the same width (0.6 mm) but with a variety of length ($0 < l \leq 65\,\text{mm}$) and orientation ($0 \leq \theta \leq 180^\circ$) generated by a random function. All parameters, as summarized in Table 1, were input to the parameterized modeling program for automated mesh generation. The size of eight-node solid elements in the plate plane was set to be 1 mm, and two layers of elements were modeled through the thickness (1.6 mm), which is adequate for

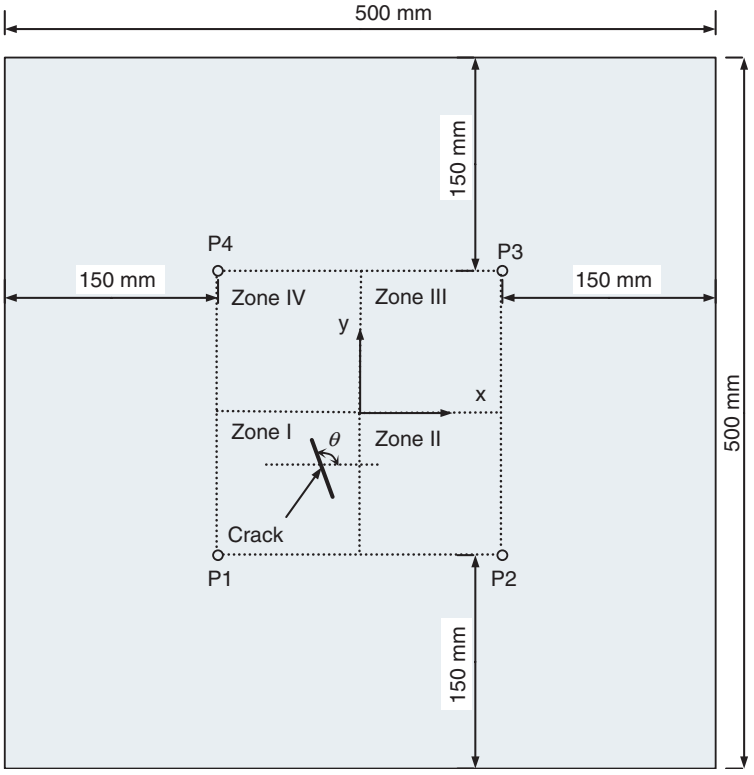

Figure 1. *Configuration of specimen and PZT discs in FEA modeling and experiments.*

Table 1. Parameters considered in FEA modeling.

Specimen	Crack	PZT disc	FEA parameters	Load case	Others
Length, width, thickness	Position, length, width, orientation	Number, position, size	Mesh density, element type	Load type, corresponding nodes	Boundary condition, material properties

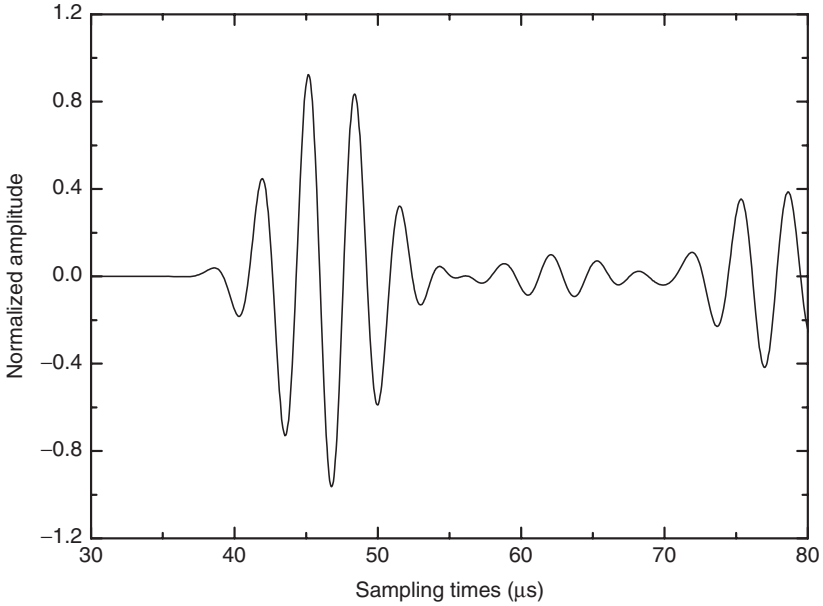

Figure 2. *Typical Lamb wave signal acquired in FEA.*

describing the characteristics of Lamb waves at a low product range of frequency and plate thickness, where the mode shapes of Lamb waves through the thickness are quite simple (Diligent and Lowe, 2005).

Three-dimensional dynamic simulation for each crack case was subsequently conducted using ABAQUS/EXPLICIT® code. A five-cycle toneburst modulated with a Hanning window at a central frequency of 0.3 MHz was imposed, as in-plane shear force, on the nodes along the radial direction of the simulated PZT actuators P1–P4 in turn (Yang et al., 2006). Lamb wave signals were collected by the other three PZT discs as sensors at a sampling frequency of 20.48 MHz (Yang et al., 2006). The acquired wave signal via actuator–sensor path P1-P2 from simulation is displayed in Figure 2 for a typical crack case. Twelve actuator–sensor paths were therefore involved for each crack case for further extraction of characteristics, which provided exclusive parameter information for individual crack cases.

DIGITAL DAMAGE FINGERPRINTS AND DAMAGE PARAMETER DATABASE

The raw Lamb wave signals were decomposed into multiple frequency regions via discrete wavelet analysis (db10, Daubechies wavelet 10). The relevant level comprising the excitation frequency (0.3 MHz in this study) was selected, and noise from other frequency bands was filtered out. Previous studies substantiated that Lamb wave signals with a dominant S_0 mode at the excitation frequency of 0.3 MHz show the best sensitivity to a through-thickness crack (Lu et al., 2007, 2008). In reconstructed wave signals, the point of time at which the magnitude of signal amplitude is larger or smaller than those of its contiguous neighbors can be marked as a 'characteristic point' and its corresponding amplitude is denoted as the 'characteristic amplitude' (Su and Ye, 2005a,b), as depicted in Figure 3. These items are recorded as principal components of the signals whereas the others are 'non-characteristic components', which are eliminated to accomplish efficient data compression.

It is presumed that any possible damage in a structure presents unique characteristics in wave signals. The extracted principal components originating from all available actuator–sensor paths in a sensor network can be assembled to form a feature pattern, called DDFs, exclusively portraying the mutual relation between distinctive changes in the characteristics of Lamb wave signals and damage parameters. For a typical crack case, the normalized principal components assembled as DDFs are schematically illustrated in Figure 4,

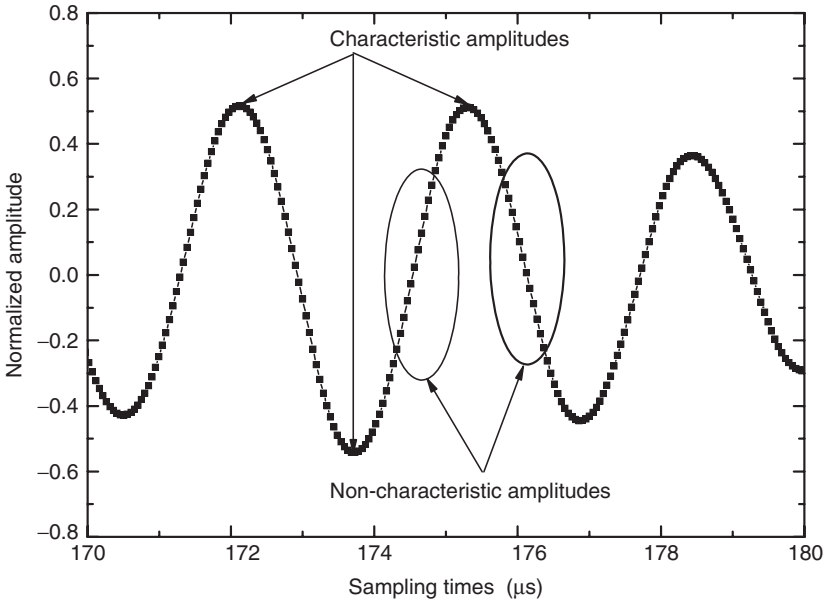

Figure 3. *Principal components vs. non-characteristic components in signal fraction.*

implicitly correlating with the parameters of the crack (location, size, and orientation).

A DPD, comprising DDF vectors extracted from randomly selected crack scenarios, can be subsequently developed as a library. A well trained ANN with the DPD can thus be used to predict a crack of unknown parameters with the DDFs experimentally acquired from a sensor network, as a typical inverse analysis. In this study, a total of 50 randomly selected crack cases with different parameters were numerically simulated for a defective plate, based on the concept of an orthogonal array (OA), to achieve a good training result (Chang et al., 2000).

Given that the specimen geometry and actuator/sensor positions are symmetrical with regard to the horizontal and vertical axes of the coordinate system in Figure 1, the available DDFs in the other quadrants can be mapped onto the quadrant of interest (Su and Ye, 2005a,b). As an example, according to the procedure in Table 2, the actuator–sensor path for one crack case in Zones II–IV can be mapped to the corresponding path for a crack with mirrored position and orientation in Zone I. It is noteworthy that the angle of the mapped crack from Zone II or IV into Zone I is changed to its supplementary angle. Without losing generality and sacrificing the amount of information about crack scenarios, redundant modeling and calculation can thus be avoided with the information mapping technique.

As a result, four parallel DPDs for the four quadrants respectively can be constructed with the vectors of the DDFs extracted from crack scenarios originally in the quadrant and those mirrored into it. However, it should be noted that successful application of the information mapping is on the basis of geometrical symmetry and the high quality of FEA modeling for various crack cases, which guarantees the equivalence of wave signals collected via different actuator–sensor paths.

ANN TRAINING AND PERFORMANCE

Feedforward ANN Model and Backpropagation Training

It has been demonstrated that ANN models with two hidden layers are adequate in most structure-related analysis for damage identification (Su, 2004). As one of the most used models, the feedforward network has information passed through the network in the forward direction with the connections of neurons between adjacent layers (Staszewski et al., 2004). As illustrated in Figure 5, such an ANN model for damage identification features one input layer with DDFs $\bar{i}_p (p = 1, \ldots, m)$, two processing (hidden) layers containing j and k neurons respectively, and one output layer with the damage parameters $\bar{o}_s (s = 1, \ldots, n)$ to be correlated. The neurons are joined to each other via the weight matrix and a set of biases. Mathematically, the sth output parameter in the designed ANN model is calculated by:

$$\bar{o}_s = F_3\left(\left(\sum_{q=1}^{k} \bar{w}^3_{q-i} \cdot F_2\left(\left(\sum_{r=1}^{j} \bar{w}^2_{r-q} \cdot F_1\left(\left(\sum_{p=1}^{m} \bar{w}^1_{p-r} \cdot \bar{i}_p\right) + \bar{b}^1_r\right)\right) + \bar{b}^2_q\right)\right) + \bar{b}^3_i\right) \quad (1)$$

where $\bar{w}^{\,l}_{u-v} (l = 1, 2)$ represents the weight connecting the uth neuron in the lth layer and the vth neuron in the $(l+1)$th layer, while $\bar{b}^{\,l}_v$ and $ni^{\,l}_v$ are the added bias and the

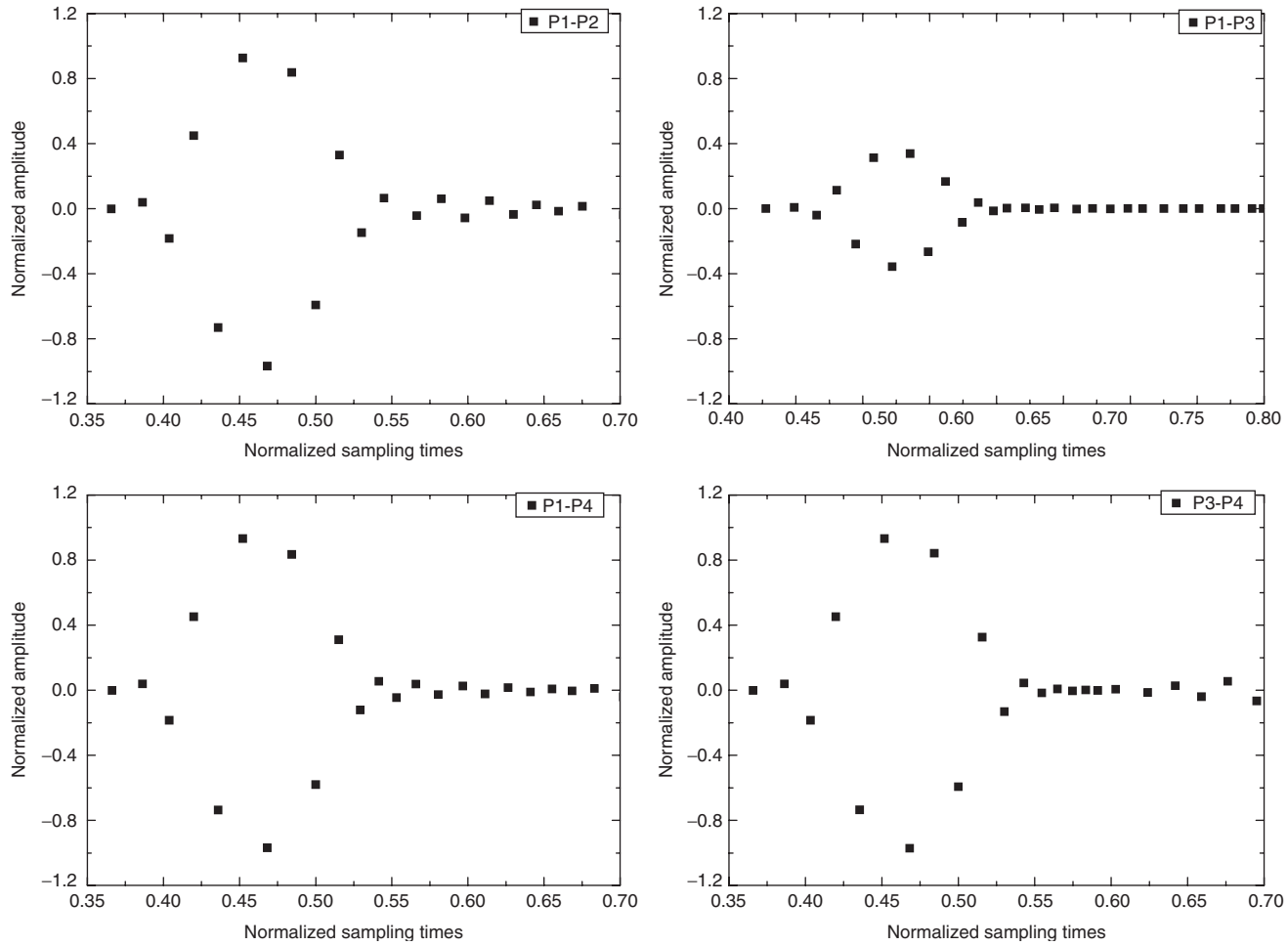

Figure 4. *DDFs composed by extracted principal components in a sensor network. (With the actuator-sensor path marked at the top-right corner of the graph.)*

Table 2. Mapping of actuator–sensor paths from other quadrants to Zone I.

	Zone II	Zone I	Zone III	Zone I	Zone IV	Zone I
Actuator–sensor path	P1-P2	P2-P1	P1-P2	P3-P4	P1-P2	P4-P3
	P1-P3	P2-P4	P1-P3	P3-P1	P1-P3	P4-P2
	P1-P4	P2-P3	P1-P4	P3-P2	P1-P4	P4-P1
	P2-P1	P1-P2	P2-P1	P4-P3	P2-P1	P3-P4
	P2-P3	P1-P4	P2-P3	P4-P1	P2-P3	P3-P2
	P2-P4	P1-P3	P2-P4	P4-P2	P2-P4	P3-P1
	P3-P1	P4-P2	P3-P1	P1-P3	P3-P1	P2-P4
	P3-P2	P4-P1	P3-P2	P1-P4	P3-P2	P2-P3
	P3-P4	P4-P3	P3-P4	P1-P2	P3-P4	P2-P1
	P4-P1	P3-P2	P4-P1	P2-P3	P4-P1	P1-P4
	P4-P2	P3-P1	P4-P2	P2-P4	P4-P2	P1-P3
	P4-P3	P3-P4	P4-P3	P2-P1	P4-P3	P1-P2

net input in the lth layer for the vth neuron in the $(l+1)$th layer. $F_l(l=1,2,3)$ is the transfer function for activating neurons in different layers (Mathworks Inc., 2001).

As one of the best known supervised learning approaches, backpropagation (BP) is associated with a stochastic steepest descent algorithm for ANN training within a required error tolerance. In detail, the mean square error function (MSE) E_r is defined as (Mathworks Inc., 2001):

$$E_r = \frac{1}{n}\sum_{s=1}^{n}\left(\bar{t}_s - \bar{o}_s\right)^2 \tag{2}$$

where $\bar{t}_s$ is the sth target vector, as shown in Figure 5. In the present study, $n=4$ and $\bar{t}_s$ corresponds to the coordinates of crack center, crack size, and crack orientation. A matrix with 50 columns symbolizing a total of 50 crack scenarios was allied as an input layer for ANN training. In the training process, the weight or bias was modified based on the steepest descent method so as to minimize the error E_r (Suh et al., 2000). The input and target data were normalized into the range $[-1, 1]$, and the weights and biases were accordingly initialized to small random values with zero-mean.

The appropriate selection of neuron numbers is generally a rule of thumb, decided by the nature of the problem. One suggested criterion is that the neuron

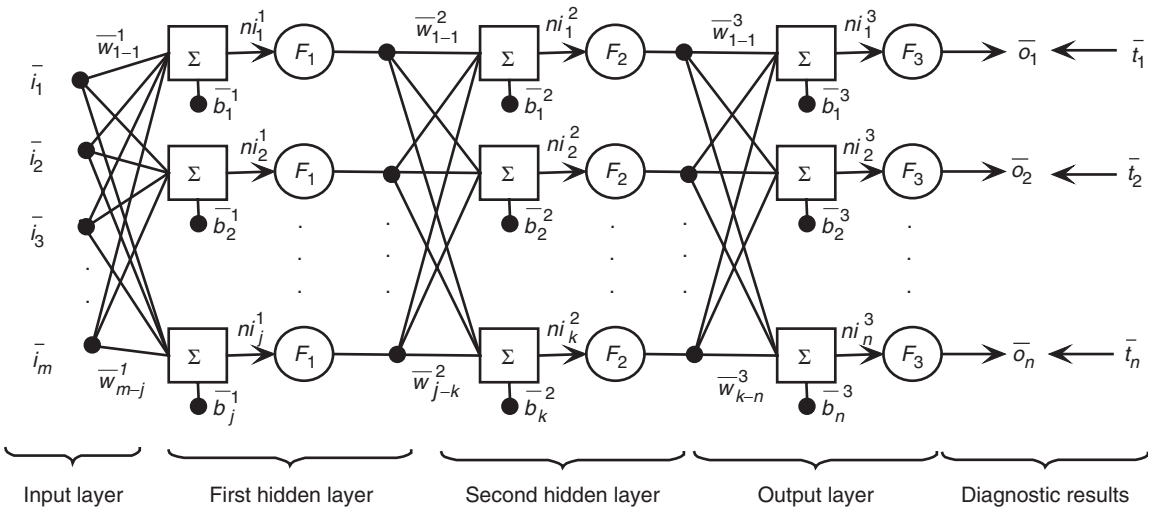

Figure 5. *Feedforward ANN model with two hidden layers.*

numbers can be approximately determined by (Su and Ye, 2005b):

$$i = \sqrt{p+q} + B \tag{3}$$

where i, p, and q are the number of neurons, input elements, and output elements for each hidden layer, respectively. B is an empirical constant ranging from 4 to 8, depending on different applications. For the current case, a neural network model designated as ANN1 was configured with the neuron numbers for the first and second hidden layers as 32 and 12, respectively.

The network training was performed using the 'Neural Network Toolbox' of Matlab (version 4.0) (Mathworks Inc., 2001). Tan-sigmoid and log-sigmoid transfer functions (Mathworks Inc., 2001) were applied between the input and first hidden layers, and the first and second hidden layers, respectively. The linear transfer function was selected for the second hidden and output layers so as to avoid the situation that the output values are limited to a small range (Zhang and Friedrich, 2003). The scaled conjugate gradient (SCG) algorithm was chosen for network training because of its excellent performance in reaching the target and convergence (Su, 2004). As plotted in Figure 6, an exponentially accelerated performance is exhibited in convergence history with an increase in iteration step, with a plateau indicating that the stabilization and saturation have been reached.

Evaluation of ANN Generalization

Generalization is one of the most important capacities of a neural network, demonstrating the potential of a well-trained neural network to approximate or predict target values with input vectors that are not in the training set (Sarle, 1997). Generalization is particularly sensitive to the number of neurons in the hidden layers. Too few neurons lead to underfitting, whereas too many neurons can cause overfitting (Mathworks Inc., 2001). Under the latter circumstance, the neural network would generate excessively complex functions to memorize all the training examples well, but it might be incapable of generalizing to new situations that are not included in the training set (Zhang and Friedrich, 2003).

Generalization can be evaluated by a process known as cross-validation, in which one from all the samples is extracted from training as a test data set to compute the MSE (Hjorth, 1994). Cross-validation is markedly superior for small data sets and can be applied for selecting the number of neurons in hidden layers or for optimizing a subset as ANN input (Sarle, 1997). In this study, one of the 50 DDF sets was selected in turn as a test data set and the other 49 DDF sets were used for network training, accomplishing a process of 'leave-one-out' cross-validation, which is advantageous for estimating the generalization of a neural network with continuous error functions such as MSE (Kohavi, 1995; Sarle, 1997).

Another neural network model with 40 and 14 neurons in the two hidden layers, referred to as ANN2, was established for the purpose of comparison. The other parameters for ANN training were set to be identical. The MSE was used to estimate the generalization quality of proposed neural networks. From the statistical histogram of the MSE in Figure 7, over 70% of crack cases are predicted satisfactorily by both ANN1 and ANN2 with the MSE value <0.1, which is 10% of the normalized maximum of target vectors. Therefore, both neural networks demonstrated good capability of generalization to new situations. On the other hand, the MSE distribution was quite stable and no obvious improvement in prediction accuracy was found with an increase in the number of neurons.

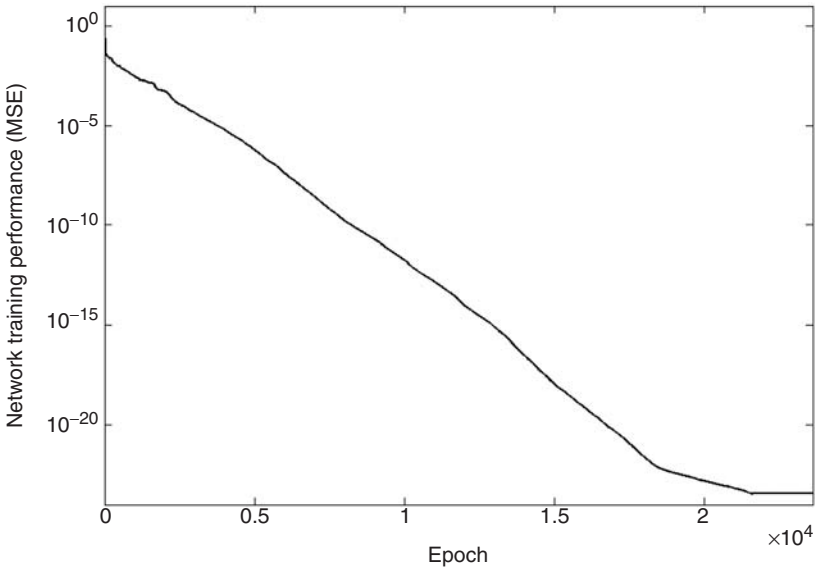

Figure 6. *Convergence history of ANN training.*

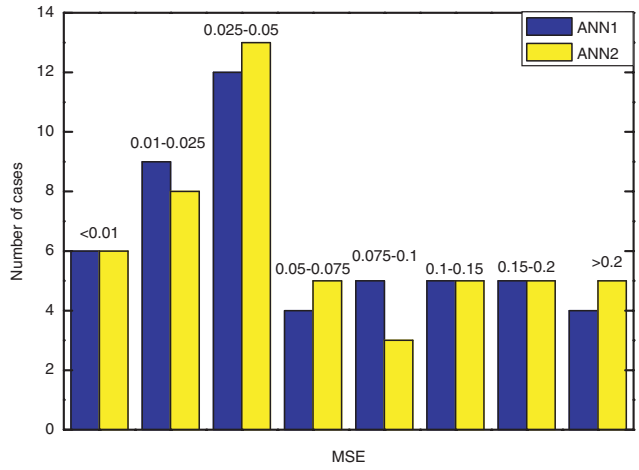

Figure 7. *Comparison of ANN generalization with different configurations.*

On the basis of these observations, it can be summarized that the proposed neural networks trained with the 50 crack cases were sufficient to portray the implicit relation between the DDFs and the crack parameters. A more complex neural network with more neurons might be unnecessary for this problem and may lead to overfitting with weak generalization capability and enormous calculation cost.

RESULTS AND DISCUSSION

Two aluminum plates with the same geometry, mechanical properties, and boundary condition as in the simulations were used to experimentally validate the performance of the well-trained neural networks. Four PZT discs were bonded using adhesive epoxy at positions on the upper surface of the plates consistent with the numerical simulations. Two through-thickness cracks with the parameters listed in Table 3, which were not included in the data set for the ANN training, were introduced by a 0.6 mm thick blade, one in each aluminum plate. With the same configuration as in the simulations, actuators P1–P4 were excited separately to generate Lamb waves and the other discs acted as sensors to acquire wave signals. These two crack cases were also calculated using FEA simulations as references.

Table 3. Parameters of cracks in two aluminum plates in experiments.

	Central position	Length	Angle
Crack I	(−12 mm, −25 mm)	30 mm	95°
Crack II	(26 mm, 15 mm)	35 mm	160°

Two sets of DDFs experimentally extracted from 12 paths of the active sensor network on two plates were therefore individually fed into the neural networks as an input vector to predict crack parameters that were unknown to the neural network beforehand. The triangulation tracing method was applied first to determine the quadrant where the crack existed (Lu et al., 2006). With this approach, Cracks I and II were initially located in Quadrants I and III, respectively. Subsequently, the trained neural networks (ANN1 and ANN2) with DPDs constructed for Quadrants I and III exclusively were evoked to provide detailed crack parameters. The diagnostic results are summarized in Table 4 and compared with the actual cracks in Figure 8, where the corresponding zones are magnified. The dashed lines schematically represent the crack cases involved for ANN training while the solid lines correspond to the prediction results of different neural networks. The results based on

Table 4. Diagnostic results of ANN1 and ANN2 for crack parameters.

			Central position	Length	Angle
Crack I		Crack parameter	(−12.00 mm, −25.00 mm)	30.00 mm	95°
	ANN1	DDFs (Experiment)	(−2.84 mm, −31.29 mm)	45.25 mm	80.3°
		DDFs (FEA)	(−11.66 mm, −27.96 mm)	32.72 mm	75.6°
	ANN2	DDFs (Experiment)	(−4.70 mm, −30.15 mm)	44.08 mm	73.2°
		DDFs (FEA)	(−11.98 mm, −28.75 mm)	32.55 mm	72.7°
Crack II		Crack parameter	(26.00 mm, 15.00 mm)	35.00 mm	160°
	ANN1	DDFs (Experiment)	(18.43 mm, 20.46 mm)	36.67 mm	121.2°
		DDFs (FEA)	(27.66 mm, 15.35 mm)	41.06 mm	133.8°
	ANN2	DDFs (Experiment)	(20.93 mm, 23.34 mm)	34.44 mm	124.2°
		DDFs (FEA)	(27.28 mm, 15.90 mm)	41.47 mm	133.2°

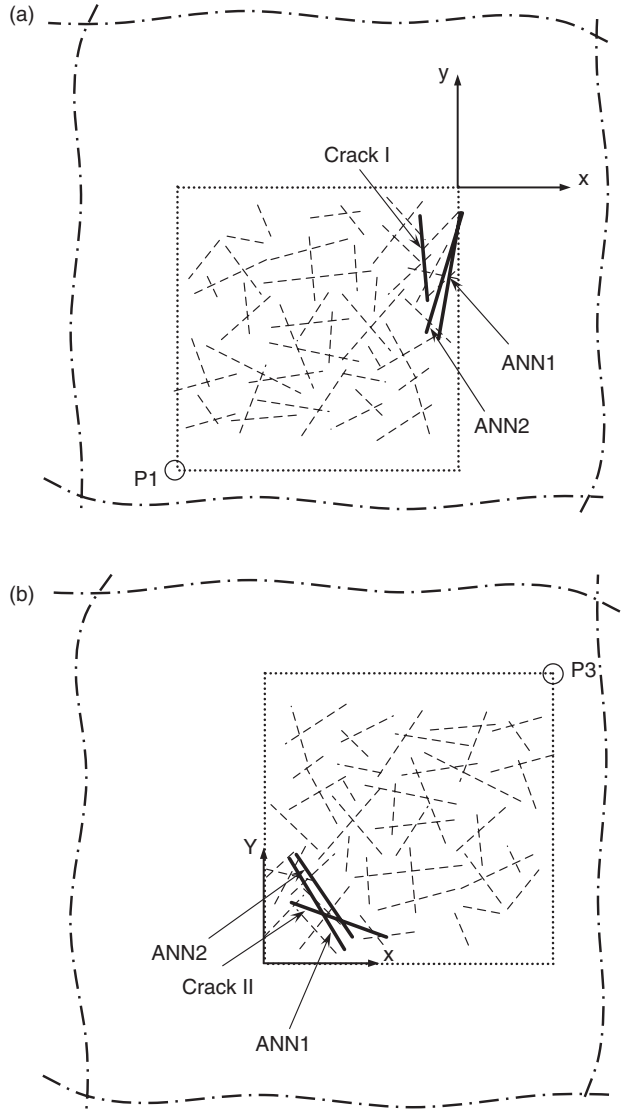

Figure 8. *Schematic illustration of results from ANNs (1 and 2) based on the DDFs extracted from experiments (a) for Crack I and (b) for Crack II.*

the DDFs extracted from the parallel numerical simulation are also listed in Table 4 for comparison.

The prediction results indicate that quantitative evaluation for crack location, size, and orientation can be achieved using the proposed ANN technique. No substantial improvement in prediction accuracy is observed with an increase in the number of neurons. The overall error in prediction for the experimental cases is greater than that for the numerical cases. This is mostly attributable to inevitable differences between numerical simulation and experimental measurement, rather than to error from the network training. Other factors also affect the accuracy for crack identification, e.g., the selection of different signal processing method (wavelet transform in this study). Nevertheless, the prediction errors of both neural networks still fall in a reasonable range, considering that the ratio of crack size to specimen dimension is <8%.

In addition to the number of neurons in the hidden layers, the performance of a neural network is strongly related to the data size of the input layer, that is, the amount of DDFs from actuator–sensor paths in each crack case, and the amount of crack cases involved for training. To investigate network sensitivity to the size of training data, a neural network (ANN3) was configured with 50 crack cases but with limited DDFs from six actuator–sensor paths where P1 and P2 were excited as actuators only. Meanwhile, two neural networks, designated as ANN4 and ANN5 respectively, were established with the DDFs from 12 actuator–sensor paths but with 20 and 40 randomly selected crack cases individually from the full DPD.

Alternatively, based on the MSE distribution of crack cases in 'leave-one-out' cross-validation, a better subset of training data can be extracted to further improve the generalization performance of a designed neural network (Sarle, 1997). A neural network designated as ANN6 was therefore established by selecting 40 crack cases as an optimal subset for ANN training, after deleting the 10 crack cases with the greatest MSEs judged in cross-validation. The neuron numbers in the

two hidden layers of ANN3–ANN6 were 32 and 12, respectively identical to the configurations of ANN1. The network configurations of ANN1–ANN6 are summarized together in Table 5.

The prediction results for the two cracks by ANN3–ANN6 are listed in Table 6 and schematically compared with the actual cracks in Figure 9, where the results from ANN3 are not included. The results based on the DDFs extracted from parallel numerical simulation are also listed in Table 6. From the results of ANN3, it is evident that the DDFs from six actuator–sensor paths are insufficient to estimate all crack parameters, although some parameters might be determined effectively. Compared with the prediction of ANN1 and ANN2, the results of ANN4 and ANN5 with fewer crack cases are considerably poorer, whereas ANN6 based on cross-validation optimization exhibits improved prediction accuracy over ANN1 for both cracks, especially for the estimation of crack orientation.

Table 5. Network configurations of ANN1–ANN6 for crack prediction.

	Crack cases for ANN training	Number of neurons in the first hidden layer	Number of neurons in the second hidden layer	Number of DDFs for each crack case
ANN1	50	32	12	528
ANN2	50	40	14	528
ANN3	50	32	12	264
ANN4	20	32	12	528
ANN5	40[a]	32	12	528
ANN6	40[b]	32	12	528

[a]Randomly selected from 50 crack cases.
[b]Optimally selected from 50 crack cases based on the MSE in cross-validation.

CONCLUSIONS

Inverse ratiocination for crack identification in aluminum plates was developed by virtue of the ANN technique, whose generalization capacity was investigated with a process of 'leave-one-out' cross-validation. A parameterized modeling program for FEA modeling was applied for cost-effective simulation of crack cases, and an information mapping technique was adopted on the basis of geometrical symmetry and high quality of FEA modeling. Using well-trained neural networks configured with the concepts of DDFs and DPD, the estimation of crack parameters was achieved with good accuracy.

It is noted that the diagnostic efficiency and precision are highly dependent on the network architecture. The following conclusions can be drawn:

1. A feedforward neural network with two hidden layers using a SCG-based BP algorithm demonstrates good capacity and capability to map the implicit relation between the DDFs and crack parameters;
2. Fifty crack cases in one-fourth of the area enclosed by four PZT sensors provide sufficient patterns with affordable computational cost;
3. Four PZT sensors, which are integrated as a standard unit of an active sensor network, provide appropriate DDFs for ANN training and quantitative crack evaluation;
4. 'Leave-one-out' cross-validation is a robust and elaborate approach for evaluating network generalization, providing an option for optimizing a data subset as an input layer, so as to prevent overfitting that could jeopardize the performance of the proposed network.

Table 6. Diagnostic results for cracks by different neural networks.

			Central position	Length	Angle
Crack I		Crack parameter	(−12.00 mm, −25.00 mm)	30.00 mm	95°
	ANN3	DDFs (Experiment)	(−18.27 mm, −0.63 mm)	50.10 mm	N/A
		DDFs (FEA)	(−16.99 mm, −20.12 mm)	35.10 mm	96.9°
	ANN4	DDFs (Experiment)	(−32.54 mm, −23.32 mm)	44.32 mm	76.4°
		DDFs (FEA)	(−40.00 mm, −20.57 mm)	62.91 mm	147.2°
	ANN5	DDFs (Experiment)	(−11.15 mm, −10.87 mm)	45.52 mm	79.7°
		DDFs (FEA)	(−13.68 mm, −26.98 mm)	33.09 mm	69.3°
	ANN6	DDFs (Experiment)	(−10.93 mm, −26.37 mm)	45.86 mm	74.6°
		DDFs (FEA)	(−15.94 mm, −22.34 mm)	31.26 mm	85.3°
Crack II		Crack parameter	(26.00 mm, 15.00 mm)	35.00 mm	160°
	ANN3	DDFs (Experiment)	(33.35 mm, 19.90 mm)	N/A	130.5°
		DDFs (FEA)	(26.11 mm, 16.38 mm)	42.42 mm	134.3°
	ANN4	DDFs (Experiment)	(26.92 mm, 9.61 mm)	54.18 mm	142.8°
		DDFs (FEA)	(22.31 mm, 15.73 mm)	41.15 mm	162.8°
	ANN5	DDFs (Experiment)	(18.90 mm, 14.12 mm)	33.09 mm	62.1°
		DDFs (FEA)	(29.03 mm, 13.41 mm)	40.14 mm	149.2°
	ANN6	DDFs (Experiment)	(31.70 mm, 14.82 mm)	35.61 mm	145.3°
		DDFs (FEA)	(29.17 mm, 14.02 mm)	40.69 mm	155.6°

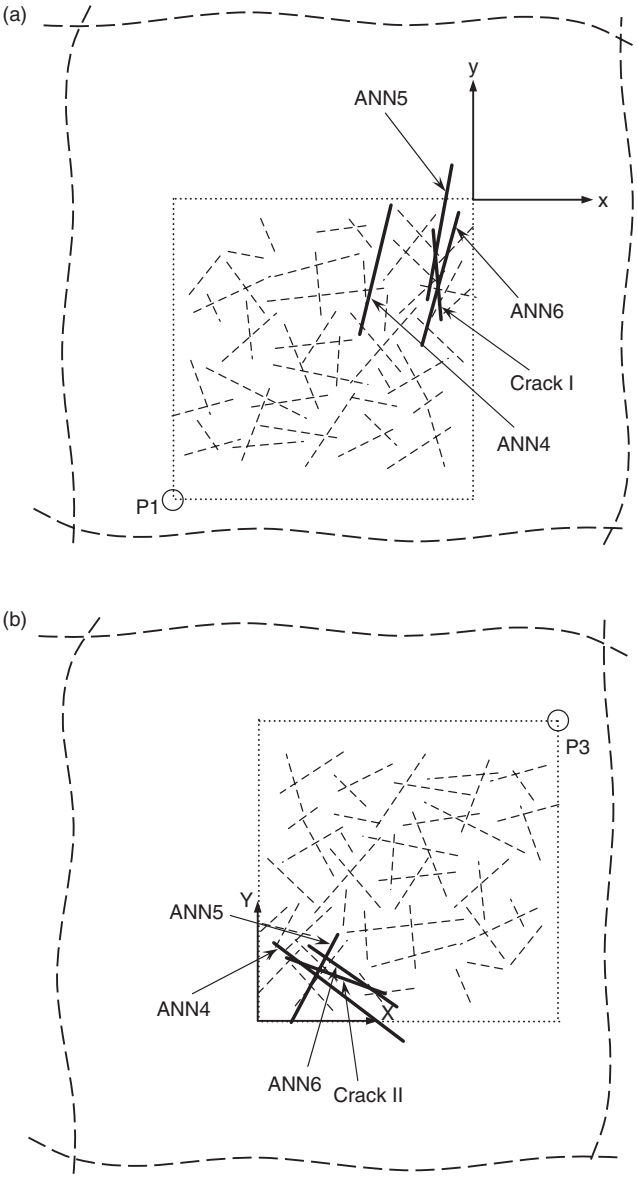

Figure 9. *Schematic illustration of results from ANNs (3-6) based on the DDFs extracted from experiments (a) for Crack I and (b) for Crack II.*

ACKNOWLEDGMENTS

One of the authors, Y.L. is supported by an International Postgraduate Research Scholarship (IPRS) from the Department of Education Science and Training (DEST), Australia, and an International Postgraduate Award (IPA) from the University of Sydney. The authors are also grateful for the Hong Kong Polytechnic University Research Grants G-U204 and A-PA8G, respectively. L.Y. is grateful for the research project grants of a Discovery Project (DP) from the Australian Research Council.

REFERENCES

Chang, C.C., Chang, T.Y.P., Xu, Y.G. and Wang, M.L. 2000. "Structural Damage Detection using an Iterative Neural Network," *Journal of Intelligent Material Systems and Structures*, 11:32–42.

Choubey, A., Sehgal, D.K. and Tandon, N. 2006. "Finite Element Analysis of Vessels to Study Changes in Natural Frequencies due to Cracks," *International Journal of Pressure Vessels and Piping*, 83(3):181–187.

Demma, A., Cawley, P., Lowe, M.J.S. and Roosenbrand, A.G. 2003. "The Reflection of the Fundamental Torsional Mode from Cracks and Notches in Pipes," *Journal of the Acoustical Society of America*, 114(2):611–625.

Diligent, O. and Lowe, M.J.S. 2005. "Reflection of the S_0 Lamb Mode from a Flat Bottom Circular Hole," *Journal of the Acoustical Society of America*, 118(5):2869–2879.

Hjorth, J.S.U. 1994. *Computer Intensive Statistical Methods*: *Validation Model Selection and Bootstrap*, Chapman & Hall, London, New York.

Huang, N., Ye, L. and Su, Z. 2004. "Parameterised Modelling Technique & its Application to Artificial Neural Network-based Structural Health Monitoring," In: Ye, L., Mai, Y.-W. and Su, Z. (eds), *Proceedings of the Fourth Asian-Australasian Conference on Composite Materials*, pp. 999–1004, Woodhead Publishing Limited, Cambridge, England.

Hwu, C.B. and Liang, Y.C. 2001. "Hole/Crack Identification by Static Strains from Multiple Loading Modes," *AIAA Journal*, 39(2):315–323.

Kohavi, R. 1995. "A Study of Cross-validation and Bootstrap for Accuracy Estimation and Model Selection," Presented at *International Joint Conference on Artificial Intelligence* (*IJCAI*), 20–25, August, Montreal, Quebec, Canada.

Kudva, J.N., Munir, N. and Tan, P.W. 1992. "Damage Detection in Smart Structures using Neural Networks and Finite-element Analyses," *Smart Materials and Structures*, 1(2):108–112.

Liu, S.W., Huang, J.H., Sung, J.C. and Lee, C.C. 2002. "Detection of Cracks using Neural Networks and Computational Mechanics," *Computer Methods in Applied Mechanics and Engineering*, 191(25–26):2831–2845.

Lowe, M.J.S. 1998. "Characteristics of the Reflection of Lamb Waves from Defects in Plates and Pipes," In: Thompson, D. and Chimenti, D.E. (eds), *Review of Progress in Quantitative Nondestructive Evaluation*, pp. 113–120, Plenum Press, New York.

Lowe, M.J.S. and Diligent, O. 2002. "Low-frequency Reflection Characteristics of the S_0 Lamb Wave from a Rectangular Notch in a Plate," *Journal of the Acoustical Society of America*, 111(1):64–74.

Lu, Y., Ye, L. and Su, Z. 2006. "Crack Identification in Aluminium Plates using Lamb Wave Signals of a PZT Sensor Network," *Smart Materials and Structures*, 15:839–849.

Lu, Y., Ye, L., Su, Z. and Huang, N. 2007. "Quantitative Evaluation of Crack Orientation in Aluminium Plates Based on Lamb Waves," *Smart Materials and Structures*, 16:1907–1914.

Lu, Y., Ye, L., Su, Z. and Yang, C. 2008. "Quantitative Assessment of Through-thickness Crack Size Based on Lamb Wave Scattering in Aluminium Plates," *NDT & E International*, 41:59–68.

Mahmoud, M.A. and Kiefa, M.A.A. 1999. "Neural Network Solution of the Inverse Vibration Problem," *NDT & E International*, 32(2):91–99.

Mathworks Inc. 2001. *Neural Network Toolbox for Use with Matlab, User's Guide*,Version 4.

Ni, Y.Q., Wang, B.S. and Ko, J.M. 2002. "Constructing Input Vectors to Neural Networks for Structural Damage Identification," *Smart Materials and Structures*, 11:825–833.

Sarle, W.S. 1997. "Neural Network FAQ, Part 1 of 7: Introduction, Periodic Posting to the Usenet Newsgroup Comp.ai.neural-nets," URL: ftp://ftp.sas.com/pub/neural/FAQ.html

Shaw, J.K., Sirkis, J.S., Friebele, E.J., Jones, R.T. and Kersey, A.D. 1995. "Model of Transverse Plate Impact Dynamics for Design of Impact Detection Methodologies," *AIAA Journal*, 33(7): 1327–1334.

Staszewski, W.J., Boller, C. and Tomlinson, G.R. 2004. *Health Monitoring of Aerospace Structures*: *Smart Sensor Technologies and Signal Processing*, J. Wiley, New York.

Su, Z. 2004. "Elastic Wave-based Quantitative Damage Identification Technique using Active Sensor Network," *Ph.D. Dissertation*, The University of Sydney, Sydney, Australia..

Su, Z. and Ye, L. 2005a. "Lamb Wave Propagation-based Damage Identification for Quasi-isotropic CF/EP Composite Laminates using Artificial Neural Algorithm, Part I: Methodology and Database Development," *Journal of Intelligent Material Systems and Structures*, 16:97–111.

Su, Z. and Ye, L. 2005b. "Lamb Wave Propagation-based Damage Identification for Quasi-isotropic CF/EP Composite Laminates using Artificial Neural Algorithm, Part II: Implementation and Validation," *Journal of Intelligent Material Systems and Structures*, 16:113–125.

Suh, M.-W., Shim, M.-B. and Kim, M.-Y. 2000. "Crack Identification using Hybrid Neuro-genetic Technique," *Journal of Sound and Vibration*, 238(4):617–635.

Xu, B., Wu, Z., Chen, G. and Yokoyama, K. 2004. "Direct Identification of Structural Parameters from Dynamic Responses with Neural Networks," *Engineering Applications of Artificial Intelligence*, 17(8):931–943.

Xu, Y.G., Liu, G.R., Wu, Z.P. and Huang, X.M. 2001. "Adaptive Multilayer Perceptron Networks for Detection of Cracks in Anisotropic Laminated Plates," *International Journal of Solids and Structures*, 38(32–33):5625–5645.

Yang, C.H., Ye, L., Su, Z. and Bannister, M. 2006. "Some Aspects of Numerical Simulation for Lamb Wave Propagation in Composite Laminates," *Composite Structures*, 75(1–4): 267–275.

Yuan, S., Wang, L. and Peng, G. 2003. "Neural Network Method Based on a New Damage Signature for On-line Structural Health Monitoring," In: Chang, F.-K. (ed.), *Proceedings of the 4th International Workshop on Structural Health Monitoring*, DEStech Publications, Lancaster, pp. 533–540.

Yun, C.-B. and Bahng, E.Y. 2000. "Substructural Identification using Neural Networks," *Computers & Structures*, 77(1):41–52.

Zhang, Z. and Friedrich, K. 2003. "Artificial Neural Networks Applied to Polymer Composites: A Review," *Composites Science and Technology*, 63(14):2029–2044.